A comparison of satellite and shipboard gravity measurements in the Gulf of Mexico

Christopher Small* and David T. Sandwell*

ABSTRACT

Satellite altimeters have mapped the marine geoid over virtually all of the world's oceans. These geoid height measurements may be used to compute free air gravity anomalies in areas where shipboard measurements are scarce. Two-dimensional (2-D) transformations of geoid height to gravity are limited by currently available satellite track spacing and usually sacrifice short wavelength resolution. Full resolution may be retained along widely spaced satellite tracks if a one dimensional (1-D) transformation is used. Although the 1-D transform retains full resolution, it assumes that the gravity field is lineated perpendicular to the profile and is therefore limited by the orientation of the profile relative to the field. We investigate the resolution and accuracy of the 1-D transform method in the Northern Gulf of Mexico by comparing satellite gravity profiles with high quality shipboard data provided by Edcon Inc. The long wavelength components of the gravity field are constrained by a low degree reference field while the short wavelength components are computed from altimeter profiles. We find that rms misfit decreases with increasing spherical harmonic degree of the reference field up to 180 degrees ($\lambda > 220$ km) with negligible improvement for higher degrees. The average rms misfit for the 17 profiles used in this study was 6.5 mGal with a 180 degree reference field. Spectral coherence estimates indicate that the satellite data resolve features with wavelengths as short as 25 km.

INTRODUCTION

In recent years, satellite altimeters have mapped the marine gravity field in remarkable detail (Haxby, 1987). Satellites such as Geos-3, Seasat, and Geosat use microwave radar to make high precision (± 2 cm vertical) measurements of the sea surface height relative to a reference ellipsoid. In the absence of disturbing forces such as tides, currents, and waves, the sea surface conforms to the geoid or gravitational equipotential surface. The short wavelength components of these geoid height profiles have been used to map fracture zones, seamounts, hotspot chains, midocean ridges and a multitude of previously undiscovered features in the worlds oceans. [See Sandwell (1991) for a review of applications.] Satellite altimeter data have also been used to map continental margin structure, particularly in remote areas where little shipboard data are available (Bostrom, 1989).

For many of these applications it is desirable to compute gravity anomalies from geoid heights so the satellite data can be compared and combined with shipboard gravity measurements. The two-dimensional (2-D) Stokes' integration formula (e.g., Heiskanen and Moritz, 1967) is commonly used to compute geoid height from the gravity anomaly, and it is straightforward to invert the Stokes formula to compute the gravity anomaly directly from geoid height. An alternate approach is to expand the geoid height in spherical harmonics, multiply each of the coefficients by a known factor, and sum the new series to construct gravity anomaly (Rapp and Pavlis, 1990; Haxby et al., 1983). From this theory it is clear that geoid height and gravity anomaly are equivalent measurements of the earth's external gravity field.

In practice, there are several problems that must be addressed when converting satellite altimeter profiles of geoid height to marine gravity anomalies. The first problem is to measure geoid height with sufficient precision to resolve short wavelength ($< \sim 100$ km) gravity anomalies. As shown below and in a previous study (Sandwell and McAdoo, 1990), such high-resolution profiles are now available from the Geosat Exact Repeat Mission (Geosat/ERM). The more severe problems are related to data coverage and sampling of the geoid height since the 2-D inverse Stokes function must be integrated over the entire surface of the earth to construct

gravity anomalies. An edge effect problem occurs because satellite altimeter measurements of geoid height are only available over ocean areas. Since the inverse Stokes kernel falls off rapidly with distance, the integration is quite accurate in the open ocean areas but becomes less accurate when gravity is computed near land. This edge effect problem can only be solved by including land gravity or geoid height measurements in the integration.

A related problem is that satellite altimeter profiles are only available along widely spaced ground tracks (Figure 1). Even when one attempts to compute the gravity anomaly along one of the satellite tracks, the recovery will be inaccurate because the 2-D integration will include points where there are no actual geoid height measurements. It is possible to interpolate the geoid height in the gaps but this reduces the accuracy and resolution of the resulting gravity values.

In the past, there have been two approaches to the recovery of gravity anomalies from local geoid height measurements. The first approach is to construct gridded gravity anomaly maps (Haxby et al., 1983; Sandwell, 1991) from an interpolated geoid height grid. Over a limited area (e.g., 4000 km × 4000 km) conversion from geoid height to gravity is most easily accomplished by first removing long wavelength components from the geoid height using a low degree spherical harmonic model, then transforming the short wavelength geoid height to gravity anomaly using a 2-D Fourier transform. This assumes that the earth is flat for length scales less than the wavelength of the highest spherical harmonic, typically 1000 km. After computing the short wavelength gravity anomaly, the long wavelength gravity anomaly from

the spherical harmonic model is replaced. As noted above, the major problem with this method is that the shortest wavelength anomalies are smoothed during the interpolation and Fourier transformation. To retain full resolution along track with the 2-D method, it is necessary to produce a grid with a cell size comparable to the along-track sampling spacing. This results in an enormous increase in computational labor to compute anomalies in the regions between tracks where there is no information. The along-track resolution may be retained more easily if a one-dimensional (1-D) transformation is applied to the profile data, thereby avoiding the smoothing inherent in the gridding process (Roest, 1987). The disadvantage is that the 1-D transformation from geoid height to gravity assumes that the gravity field is lineated perpendicular to the trackline. If, for example, a profile crosses perpendicular to the strike of a straight continental margin then the method gives the correct answer. However, if the profile crosses at some other angle, the amplitude of the calculated anomaly will be less than the true amplitude.

While the accuracy and resolution of geoid height measurements has been established for Geosat (Sandwell and McAdoo, 1990), the ability of 1-D transform techniques to compute free air gravity anomalies has not. In this study, we investigate the accuracy and resolution of the 1-D approach. This is done by comparing 17 satellite gravity profiles with conventional shipboard gravity data from the northern Gulf of Mexico. The Gulf is a particularly good area to test the 1-D method because an extremely high quality shipboard data set has been compiled by Edcon, Inc. Although the satellite data cannot equal the short wavelength resolution of
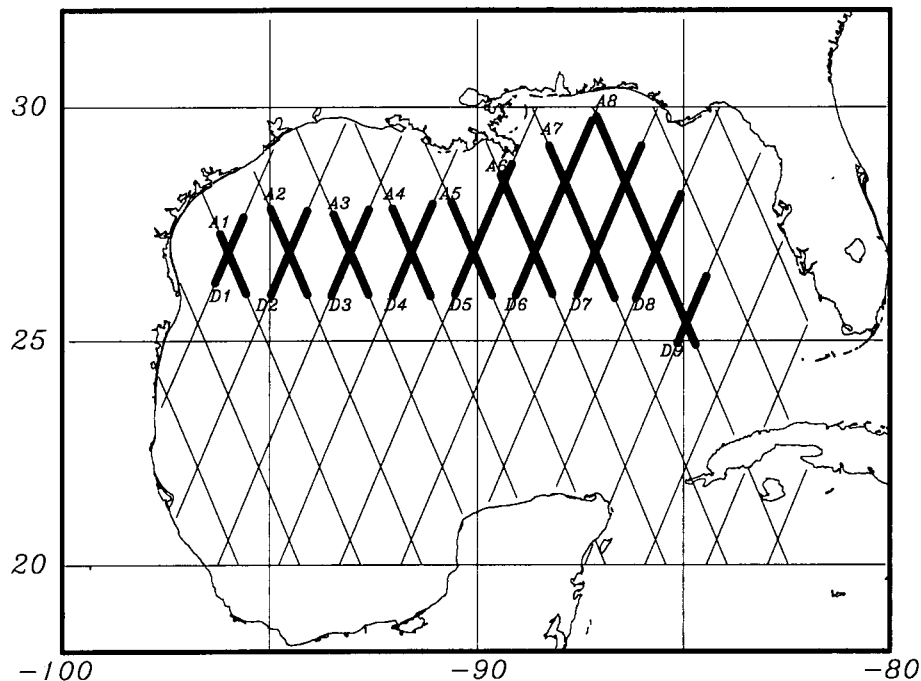

FIG. 1. Index map showing location of profiles used in this study. Long thin lines are satellite tracks with 3.4 km sampling interval. Short thick lines indicate regions of available shipboard coverage. Shipboard data are interpolated from a 6000' grid along satellite tracks with an 0.5 km sample spacing. Ascending profiles are labeled A1-A8 and descending profiles are labeled D1-D9.

the shipboard data, we obtain excellent agreements between the satellite gravity and the shipboard gravity at intermediate wavelengths (25 < λ < 500 km) if a spherical harmonic model is used as a reference field.

GEOSAT AND SHIPBOARD GRAVITY DATA

The satellite altimeter data used in this study consist of 17 profiles in the Gulf of Mexico, 8 ascending profiles (running southeast to northwest) and 9 descending profiles (running northeast to southwest). These satellite tracks are shown in Figure 1 as long, thin lines. The satellite data were collected by the Geosat spacecraft during its Exact Repeat Mission (Geosat/ERM) where every 17 days it repeated its ground track to a tolerance of ±1 km. The first 44 repeat cycles (2-years of data) were averaged to improve the accuracy and resolution of the data. This averaging procedure is described in Sandwell and McAdoo (1990), so only a brief summary is given here.

Satellite altimeter measurements of geoid height contain long wavelength orbit errors (~1 m) which greatly exceed the short wavelength precision of the measurements (~2 cm). Because of this long wavelength error, it is not possible to simply average the repeat profiles without first applying some sort of correction or high-pass filter. We adopted the high-pass filter approach where the first step in the data processing was to differentiate each profile. This effectively suppresses the long wavelength orbit error and results in sea surface slope profiles (also called vertical deflections). After differentiation, individual profiles were averaged (Figure 2, upper plot) to increase the signal-to-noise ratio and also minimize the time varying components of sea surface topography caused by unmodeled tides and ocean currents.

After averaging, the accuracy and resolution of the data were estimated by comparing repeat profiles (Sandwell and McAdoo, 1990). The uncertainty in the averaged profile was calculated as the standard deviation of the individual profiles about the mean (Figure 2, lower plot). In open ocean areas and at low latitudes, the uncertainty is generally less than 1 μrad. In enclosed bodies of water, such as the Gulf of Mexico, the uncertainty is slightly higher (~1.5 μrad) because not all of the 44 profiles are available for averaging; in this case only about 25 out of 44 are available.

The second method of estimating the accuracy of the profiles was to average one year of profiles (up to 22) and compare this average with the average for the second year. In general, these independent averages have a mean difference of less than 0.05 μrad and an rms difference of less than 1.5 μrad (Sandwell and McAdoo, 1990). The resolution of the profiles was estimated through a coherence analysis where the first year average is crosscorrelated with the second year average. Results show that over most ocean areas, these altimeter data can resolve wavelengths as short as 20 km.

The shipboard gravity data were provided by Edcon Inc. for the region shown in Figure 1 (short thick lines). The shipboard profiles were interpolated from a densely gridded gravity map having a 6000 ft (1829 m) point spacing. The grid was produced from a series of shipboard profiles collected with a LaCoste Romberg S type gravimeter. The original shipboard gravity profiles were adjusted at crossover points;

the mean crossover error for the entire grid was 1.55 mGal before correction and 0.4 mGal after correction. Based on our experience with deep ocean shipboard gravity data, these Gulf of Mexico data represent perhaps the best ocean gravity survey available. We treat these data as "ground truth" since it is expected that their accuracy and resolution are superior to the satellite altimeter profiles.

THEORY AND DATA PROCESSING

A modified version of the Fourier transform method described briefly in Haxby et al., (1983), Roest (1987), and McAdoo et al. (1990) was used to compute along-track gravity anomalies from along-track vertical deflections. To retain the along-track resolution and simplify the computations, a flat-earth approximation was used for the short wavelength part of the transformation. To retain the long wavelength accuracy of the gravity profile, a spherical
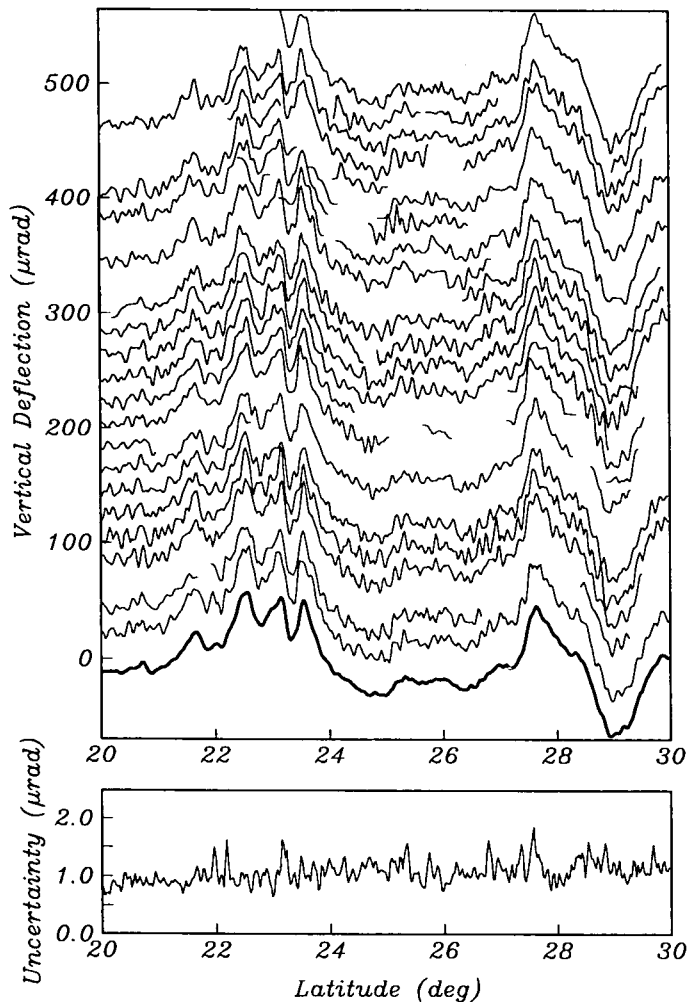

FIG. 2. Example of stacking procedure. Individual vertical deflection profiles (upper curves) are stacked to produce an average profile (heavy curve). The standard deviation at each point provides a measure of the uncertainty in the profile (bottom curve). Oceanographic effects and data gaps result in a higher than average uncertainty (~1 μRAD) FOR THIS PROFILE.

harmonic model is subtracted from the vertical deflection profiles before the along-track gravity is computed. Finally, the gravity anomaly computed from the same spherical harmonic model is added back to the along-track gravity profiles. Here we describe the 1-D transformation method in detail.

To begin, one must relate the geoid height $N(\mathbf{x})$ and other measurable quantities such as gravity anomaly $\Delta g(\mathbf{x})$ to the gravitational potential $\phi(\mathbf{x}, z)$. In the following equations, the bold $\mathbf{x}$ denotes the coordinate (x, y); similarly $\mathbf{k}$ denotes (k_x, k_y) where $k_x = 1/\lambda_x$ where λ_x is wavelength.

Using Brun's formula, we define the following quantities

— Geoid Height,

$$N(\mathbf{x}) = \frac{1}{g} \, \phi(\mathbf{x}, 0) \tag{1}$$

— Gravity Anomaly,

$$\Delta g(\mathbf{x}) = -\frac{\partial \phi}{\partial z} (\mathbf{x}, 0) \tag{2}$$

— Vertical Deflection, East Component,

$$\eta(\mathbf{x}) \equiv -\frac{\partial N}{\partial x} = \frac{-1}{g} \frac{\partial \phi}{\partial x} \tag{3}$$

— Vertical Deflection, North Component,

$$\xi(\mathbf{x}) \equiv -\frac{\partial N}{\partial y} = \frac{-1}{g} \frac{\partial \phi}{\partial y}. \tag{4}$$

These quantities are related to one another through Laplace's equation:

$$\frac{\partial^2 \phi}{\partial x^2} + \frac{\partial^2 \phi}{\partial y^2} + \frac{\partial^2 \phi}{\partial z^2} = 0. \tag{5}$$

Substitution of equations (2), (3), and (4) into Laplace's equation (5) yields

$$-g \left| \frac{\partial \eta}{\partial x} + \frac{\partial \xi}{\partial y} \right| - \frac{\partial \Delta g}{\partial z} = 0. \tag{6}$$

The derivative property of Fourier transforms along with the upward continuation property of the gravitational potential is used to reduce the differential equation (6) into an algebraic equation. The forward and inverse Fourier transforms are defined as

$$F(\mathbf{k}) = \int_{-\infty}^{\infty}\int_{-\infty}^{\infty} f(\mathbf{x}) \exp\left[-i2\pi(\mathbf{k} \cdot \mathbf{x})\right]d^2x, \tag{7}$$

$$f(\mathbf{x}) = \int_{-\infty}^{\infty}\int_{-\infty}^{\infty} F(\mathbf{k}) \exp\left[i2\pi(\mathbf{k} \cdot \mathbf{x})\right]d^2k. \tag{8}$$

The Fourier transform of equation (7) is

$$-i2\pi g[k_x \eta(\mathbf{k}) + k_y \xi(\mathbf{k})] - \frac{\partial \Delta g(\mathbf{k}, z)}{\partial z} = 0, \tag{9}$$

where g is the gravitational acceleration and i is $\sqrt{-1}$. From the solution to Laplace's equation in the wavenumber do-

main, the upward continuation formula relates the gravity anomaly at the surface of the earth to the gravity anomaly at some elevation z.

$$\Delta g(\mathbf{k}, z) = \Delta g(\mathbf{k}, 0) \exp\left[-2\pi|\mathbf{k}|z\right], \tag{10}$$

where

$$|\mathbf{k}| = (k_x^2 + k_y^2)^{1/2}.$$

Taking the derivative of equation (10) with respect to z and evaluating the result at $z = 0$, we arrive at an algebraic formula relating the Fourier transform of the gravity anomaly to the sum of the Fourier transform of the two components of vertical deflection:

$$\Delta g(\mathbf{k}, 0) = \frac{ig}{|\mathbf{k}|} [k_x \, \eta(\mathbf{k}) + k_y \xi(\mathbf{k})]. \tag{11}$$

To compute gravity anomalies from a dense network of satellite altimeter profiles of geoid height, we construct a uniform grid of geoid height and calculate the east η and north ξ components of vertical deflection. However, as mentioned above, the characteristic spacing of the Geosat profiles is much greater than the resolution along individual profiles; this limits the resolution of the resulting grid to wavelengths on the order of the track spacing. To overcome this problem, we use a 1-D approximation. First we align the x-axis of the local coordinate system in the direction of the satellite ground track. Then we assume that the curvature of the geoid in the crosstrack direction is zero; this assumption eliminates the y-derivatives in equations (5) and (6) and the k_y terms in equations (9) and (11). After simplification, the Fourier transform of the along-track gravity anomaly is related to the Fourier transform of the along-track vertical deflection by

$$\Delta g(k_x) = ig \, \frac{k_x}{|k_x|} \, \eta(\mathbf{k}). \tag{12}$$

This procedure of Fourier transformation of the along-track vertical deflection, multiplication by ig sgn (k_x), and inverse Fourier transformation corresponds to the Hilbert transform of the vertical deflection profile scaled by the average acceleration of gravity. This formula provides the gravity anomaly on a reference surface and requires an additional correction to account for the deviation of the sea surface or geoid height from the reference surface. From equation (12) we see that 1 microradian (μrad) of vertical deflection corresponds to 0.98 mGal of horizontal gravity anomaly.

The conversion of vertical deflections to free air gravity anomalies involves low-pass filtering of the data, removing the long wavelength components of the potential, Hilbert transforming the deflections to compute gravity anomaly, and then replacing the long wavelength components of the gravity field; the various steps are shown in Figure 3. This process is applied to each profile independently and makes use of the fast Fourier transform (FFT) algorithm to implement the Hilbert transform.

During the averaging of the repeat vertical deflection profiles a low-pass filter was applied (Sandwell and McAdoo, 1990). The low-pass filter operation consisted of convolution with a Gaussian function where the 0.5 attenuation occurs at

a wavelength of 18 km. This prefiltering was performed prior to averaging so that the cutoff wavelength could not be changed.

To minimize error resulting from the flat-earth approximation and any components of the field with wavelengths longer than the individual profile, a low degree geoid model is removed from the vertical deflection profiles (Figure 3, top profile). The long wavelength field was obtained from the OSU89B1 geopotential model (Rapp and Pavlis, 1990). Although this model is complete to a spherical harmonic 360 degrees, we have investigated the effect of removing lower degree fields as well. Once the vertical deflections are appropriately band limited, the Hilbert transform is applied [equation (12)]. To minimize the edge effects associated with the Fourier transformation of a finite length profile, the ends of the vertical deflection profiles are extended and the cosine tapered to zero. After the data are transformed and rescaled, the long wavelength components of the gravity field obtained from the model are replaced. The final gravity profile is shown as the lowest profile in Figure 3 along with the shipboard gravity profile for comparison. For all of these comparisons, no shifts or linear trends have been applied to either the satellite gravity profiles or the shipboard gravity profiles.
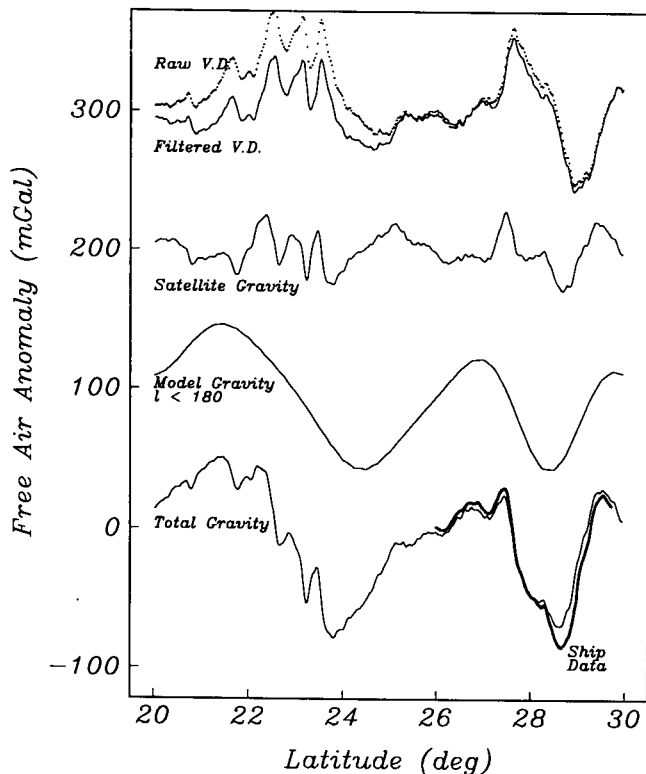

FIG. 3. Example of the processing sequence used to compute gravity profiles. Raw vertical deflections (upper dotted curve) are smoothed, and the long wavelength components of the gravity field are removed. The resulting filtered vertical deflection profile (upper solid curve) is Hilbert transformed to compute the short wavelength components of the satellite gravity profile. The long wavelength components of the gravity field are then replaced to produce the final gravity profile. Available shipboard data are shown as the darker curve for comparison.

RESULTS

The comparisons between all of the available satellite gravity profiles and shipboard gravity profiles are shown in Figure 4. In all cases the shipboard gravity profile is the solid curve and the satellite gravity is the long dashed curve. For this comparison, the OSU89B1 spherical harmonic model to 180 degrees was used as a reference field (Rapp and Pavlis, 1990). The average rms difference between the 17 satellite gravity profiles and the corresponding shipboard gravity profiles is 6.5 mGal. Also shown in Figure 4 (short dashed curve) is the 1-D satellite gravity anomaly that was constructed using no spherical harmonic reference model; in this case, the rms difference is somewhat higher (15.5 mGal). It can be seen that, in most cases, the primary effect of using the long wavelength reference model is to adjust the dc component of the profile and in some cases to correct a long wavelength trend. In general, the agreements are quite good especially at intermediate and long wavelengths ($\lambda > 25$ km). However, as expected, the short wavelength anomalies are not resolved by the satellite data.

To quantify the short wavelength resolution of the satellite data, we have estimated the spectral coherence between the satellite and shipboard gravity profiles. Spectral coherence is defined as

$$\gamma_{xy}^2(k) = \frac{|G_{xy}(k)|^2}{G_{xx}(k)G_{yy}(k)},$$

where $G_{xy}(k)$ is the cross spectrum and $G_{xx}(k)$ and $G_{yy}(k)$ are the auto spectra of data series (Bendat and Piersol, 1986). Spectral coherence estimates range from 0 to 1 for wavenumbers between 0 and the Nyquist frequency (1 km in this case) and provide a measure of the degree to which the satellite and shipboard gravity data are linearly related at a given wavenumber. Because the available shipboard profiles are relatively short and dominated by long wavelength anomalies, spectral coherence was not estimated for individual profiles. The individual profiles were tapered and concatenated to produce a single profile for the shipboard data and a single profile for the satellite data. These longer profiles are much better suited to a spectral analysis and allow for ensemble averaging, thereby reducing the variance of the spectral estimates. The spectral estimates were made using Welch's method of averaging over modified periodigrams (Welch, 1967).

The coherence estimates, with 95 percent confidence intervals are shown in Figure 5. Because the confidence intervals for coherence estimates are inversely proportional to the value of the estimate itself, the confidence intervals for the low coherences are very large and therefore not plotted. At wavelengths greater than 50 km (wavenumber <0.02 km^{-1}) the coherence between the satellite gravity and the shipboard gravity is quite high (>0.9), but it falls off sharply at shorter wavelengths; by a 25 km wavelength, the coherence is 0.5, and it is essentially zero for wavelengths less than 16 km. These resolution estimates are only slightly worse than the estimates derived from repeating Geosat/ERM profiles in deep ocean areas (Sandwell and McAdoo, 1990) suggesting that the hybrid method of computing satellite gravity anom-

alies does not significantly degrade the along-track resolution of the Geosat/ERM profiles.

Although the coherence provides a measure of the short wavelength resolution of the satellite gravity profiles, it does not provide a measure of the accuracy of the satellite data. To estimate the absolute accuracy, we calculated the rms difference between the satellite gravity profiles and the shipboard profiles. In addition, we varied the cutoff wavelength of the spherical harmonic model to establish the optimum cutoff. Six reference models were used corresponding to spherical harmonic cutoffs of 40, 90, 130, 180, 270, and 360 degrees. In each case, the spherical harmonic coefficients were tapered using a cosine function to reduce ringing in the reference gravity field. For example, the 180 degree cutoff model was tapered between harmonics of 140 and 220 degrees. As seen in Figure 6 (filled circles), the rms difference between the 17 satellite gravity profiles and the

shipboard profiles decreases with increasing spherical harmonic degree of the reference model.

DISCUSSION

In the introduction, we identified three practical reasons why it is difficult to construct gravity anomalies from satellite altimeter profiles. The first was poor altimeter resolution and accuracy, the second was an edge effect due to the lack of satellite altimeter measurements over land, and the third was the unresolved anomalies due to the wide track spacing of the Geosat/ERM profiles.

We first consider whether or not the disagreement between the shipboard and satellite measurements are a result of inaccurate satellite data. As shown in Figure 2, the uncertainty of the averaged vertical deflection profile was computed during the averaging process, and it provides a
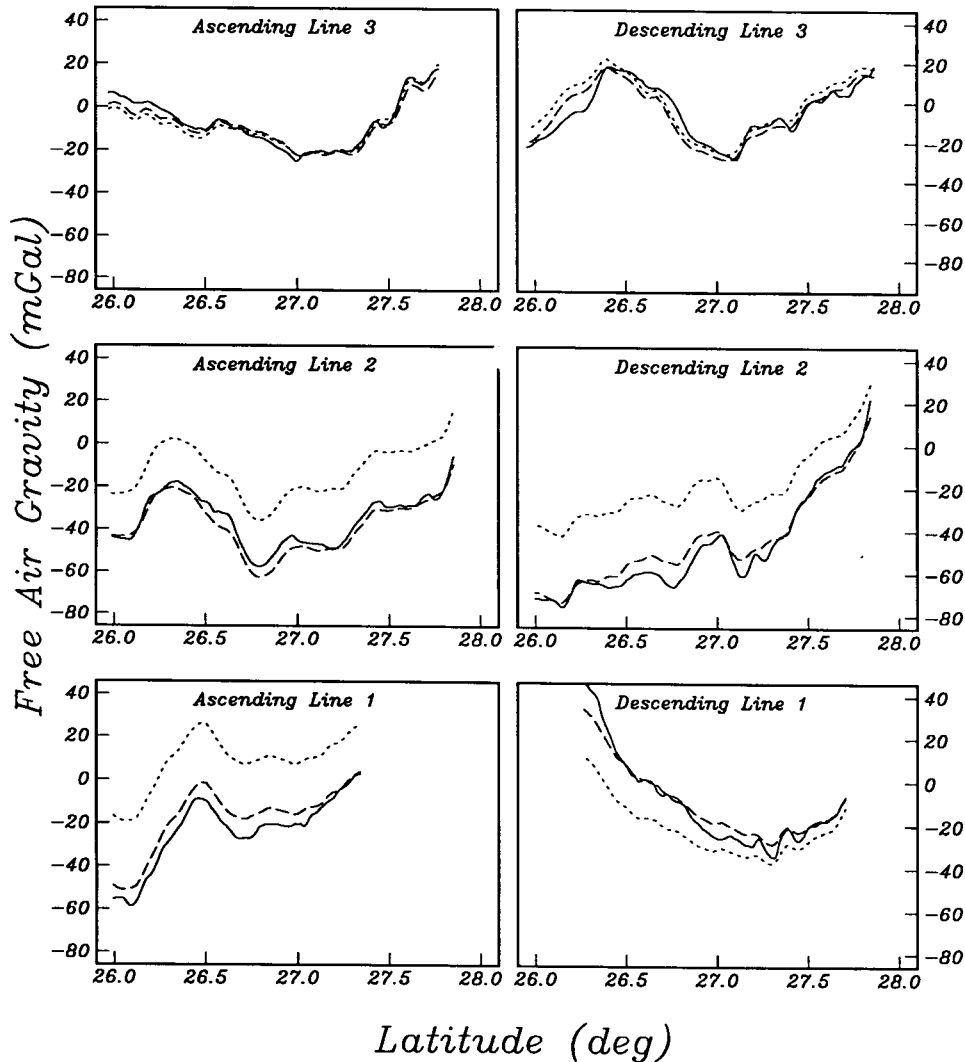

FIG. 4. Comparison of 17 shipboard and satellite gravity profiles in the northern Gulf of Mexico. Locations are shown in Figure 1. In each case, the shipboard data are plotted as the solid curve, the satellite gravity computed with a 180 degree reference field is shown as the long dashed curve, and the satellite gravity computed without a reference field is shown as the short dashed curve. The shipboard data have been decimated to 3.4 km for display purposes.

measure of the precision of the 1-D satellite gravity profiles. We have compared this estimated uncertainty with the difference between the satellite gravity and the shipboard gravity on a point-by-point basis and found no apparent correlation. We have also compared the rms misfit to the mean uncertainty for each profile and found no correlation. Since the estimated uncertainty is also four times smaller than the rms disagreement of the satellite gravity profile, we do not believe that the accuracy of the satellite measurements is the limitation.

The spectral coherence estimates in this study indicate that the satellite can resolve features with wavelengths as short as 25 km. The power spectrum of the shipboard data indicates that there is significant power at shorter wavelengths, as would be expected. Figure 7 shows an example of the difference in resolution from the northern end of descending line 3. The solid curve is the shipboard data and the dashed curve is the satellite data computed with a 180 degree reference field. The agreement with the ~20 km resolution limit for deep ocean profiles (Sandwell and McAdoo, 1990)

would seem to indicate that this is a fundamental limitation of the Geosat altimeter data. Although future satellite missions will provide tighter track spacing, altimeter precision is not expected to increase dramatically (McConathy and Kilgus, 1987). Altimeter resolution is limited by the sea state, atmospheric effects, and the noise level in the return signal which require that the data be edited and smoothed before processing. This smoothing is probably the primary limitation on the along-track resolution of the satellite data.

The fundamental assumption of the 1-D Hilbert transform is that the 2-D spectrum of the geoid slope in the across-track direction is zero [i.e., $\xi(\mathbf{k})$ in equation (11)]. This implies that the gravity field is corrugated in the direction perpendicular to the profile and is obviously a poor assumption in the Gulf of Mexico. Profiles A8 and D7 (Figure 1) illustrate this limitation. Profile D7 is nearly perpendicular to the strong gravity trough associated with the Florida Escarpment at 28° latitude (Figure 4). In this case, the 1-D approximation is nearly valid, and the satellite gravity (both with and without the reference model) match the shipboard gravity remark-

(FIG. 4. continued)

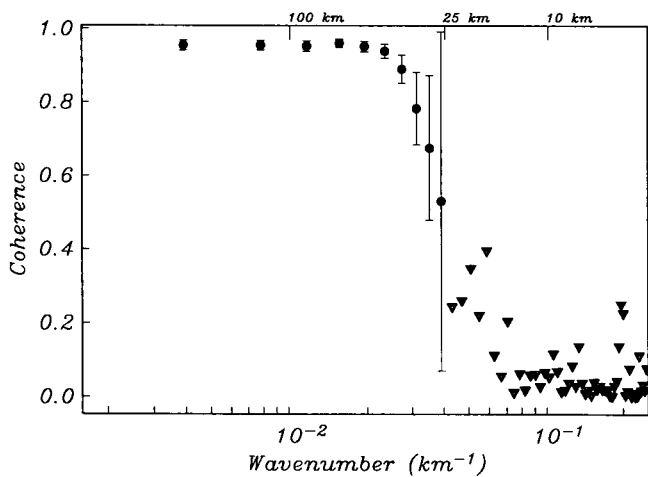*Latitude (deg)*
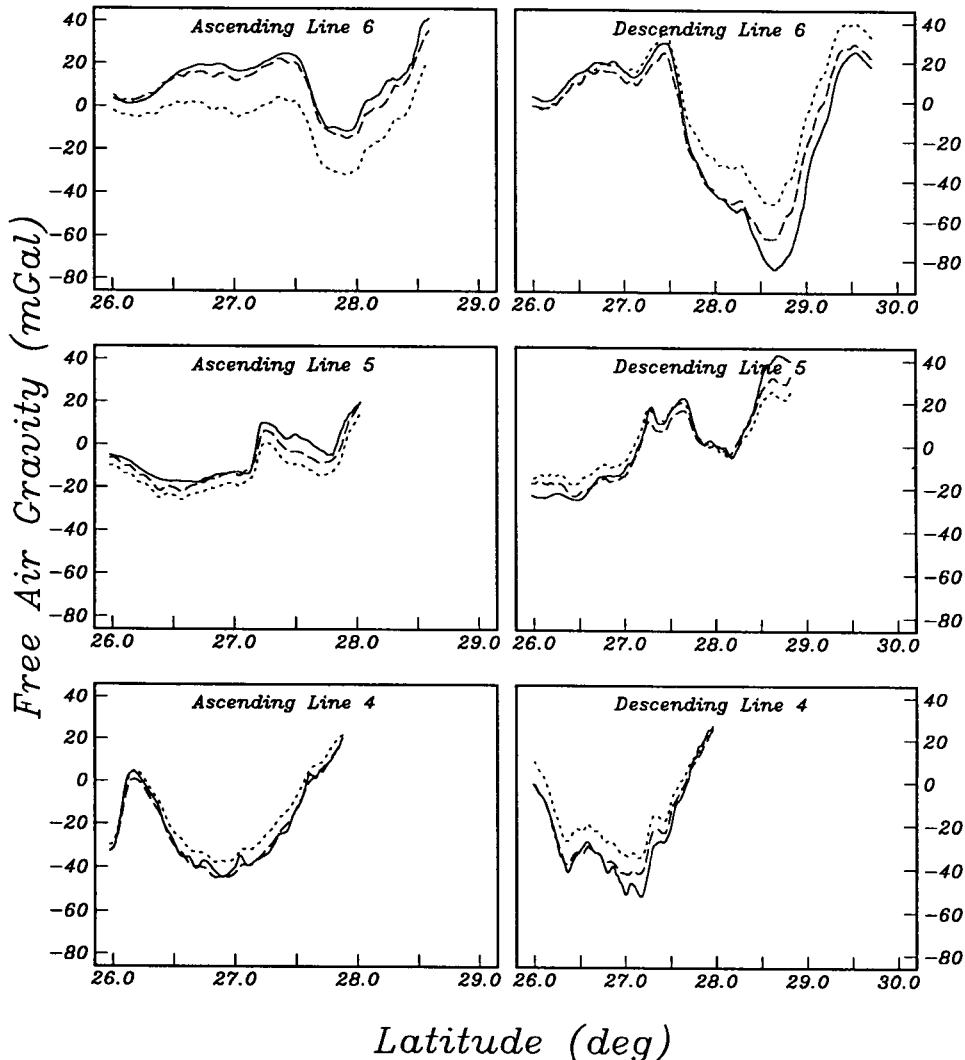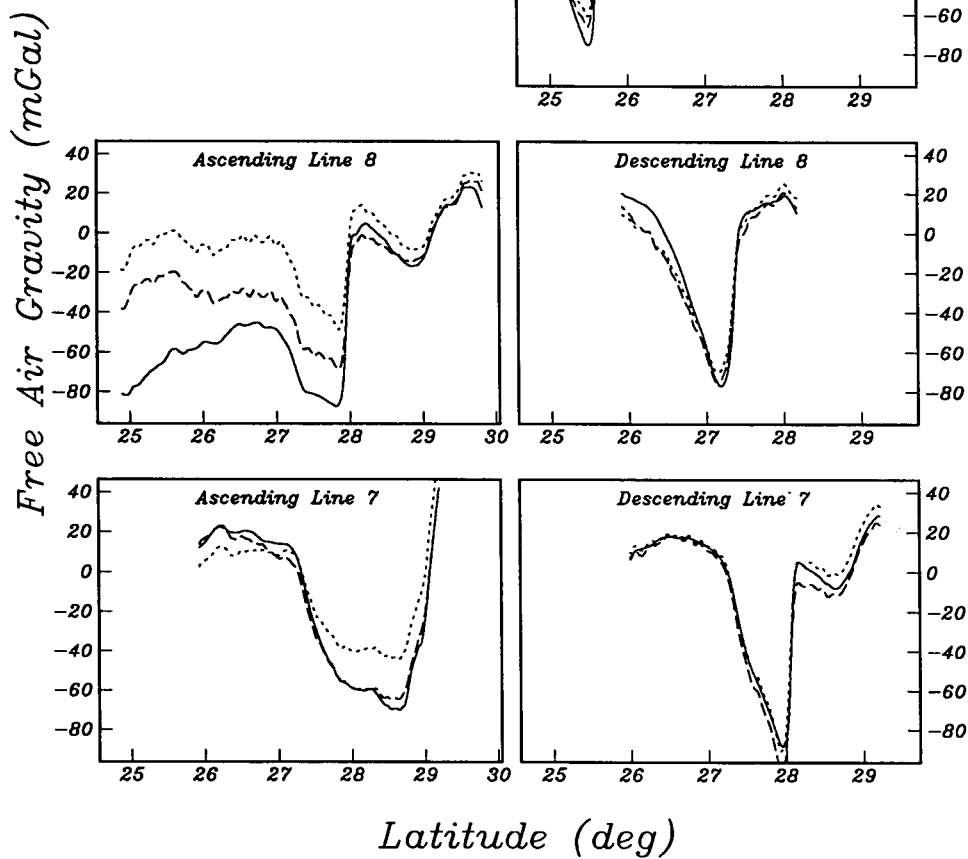
(FIG. 4. continued)

FIG. 5. Spectral coherence estimates for shipboard and satellite gravity profiles. Satellite data were interpolated to the 0.5 km sample spacing used for the shipboard data. Coherence rolls off to 0.5 at a wavenumber of 0.4 km^{-1} giving an effective resolution limit of 25 km for the satellite data. Error bars indicate 95 percent confidence intervals.
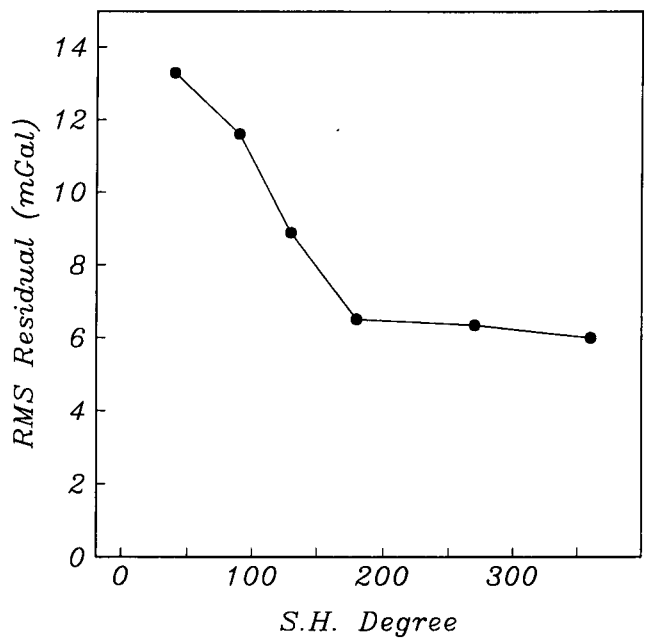
FIG. 6. RMS misfit versus spherical harmonic degree of reference field. Residual decreases linearly with the increasing degree of reference field up to 180 degrees ($\lambda > 220$ km). Improvement is negligible for 180 to 360 degrees ($\lambda > 110$ km).

ably well. In contrast, profile A8 crosses the same area of the Florida Escarpment but at an angle of ~20°. In this case, the satellite gravity profile with no reference model shows a poor fit to the shipboard profile; the amplitude of the satellite gravity step is only 2/3 the actual amplitude. The fit is improved by using the 180 degree reference, but even in this case, the satellite gravity step is too small.

Since the spherical harmonic expansion of the long wavelength gravity field is fully 2-D and correctly models the long wavelength components of the field, we assume that the 1-D assumption is the primary cause of the long wavelength disagreement seen in the uncorrected profiles. Given the rather complex nature of the gravity field in the Gulf at intermediate to long wavelengths it is not surprising that the 1-D assumption would break down at these wavelengths. Although we do not expect the short wavelength resolution to vary appreciably for other basins, the long wavelength agreement should be strongly dependent on large scale regional structure. For example, profiles crossing nearly perpendicular to a rather linear continental margin should be able to accurately reproduce wavelengths longer than 220 km without a reference field. Although an analogous 1-D transform that assumes an isotropic gravity field may be applied, we feel that this is even less justified than a lineated field in a continental margin environment.

CONCLUSIONS

In conclusion, shipboard gravity data in the Gulf of Mexico provide a "ground truth" measure of the accuracy and resolution of satellite gravity profiles. Moreover, they enable us to choose the optimum method for constructing
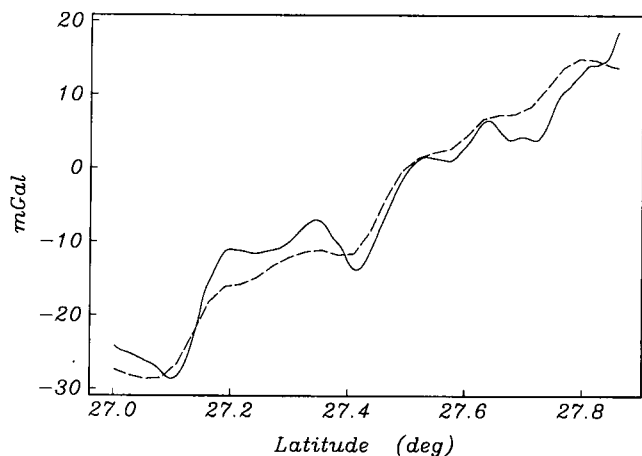

FIG. 7. The northern end of descending profile line 3 shown on an enlarged scale. The shipboard data indicated by the solid curve, and the satellite data, computed with 180 degree reference field, is shown as the dashed curve. Although the satellite resolves features with wavelengths as short as ~25 km, the amplitude is substantially reduced.

these profiles. To retain the short wavelengths available in the Geosat/ERM data and still construct accurate gravity profiles, we have developed a procedure where a spherical harmonic gravity model is used to constrain the long wavelengths, while the original satellite profile provides the short wavelength gravity signal. Spectral coherence estimates indicate that the satellite-derived gravity profiles resolve wavelengths as short as 25 km in the Gulf of Mexico. By varying the spherical harmonic degree of this reference model, we found that the accuracy in the satellite gravity profiles increases linearly as a function of the spherical harmonic up to 180 degrees; for higher degrees the improvement is negligible. When a 180 degree spherical harmonic reference model is used, the satellite gravity profiles are accurate to 6.51 mGal for wavelengths >25 km. The shipboard data show significant anomalies at shorter wavelengths that are unresolved by the satellite.

ACKNOWLEDGMENTS

REFERENCES

Bostrom, R. C., 1989, Subsurface exploration via satellite-Structure visible in Seasat images of North Sea, Atlantic Continental Margin, and Australia, AAPG Bull., **73**, 1053–1064.

Bendat, J. S., and Piersol A. G., 1986, Random data analysis and measurement procedures, Second Ed.: John Wiley & Sons, Inc.

Haxby, W. F., 1987, Gravity field of the world's oceans: Nat. Geophys. Data Center, NOAA, Boulder, CO.

Haxby, W. F., Karner, G. D., LaBrecque, J. L., and Weissel, J. K., 1983, Digital images of combined oceanic and continental data sets and their use in tectonic studies: EOS Trans. Am. Geophys. Union, **64**, 995–1004.

Heiskanen, W. A., and Moritz, H., 1967: Physical geodesy, San Francisco, Calif.: W. H. Freeman & Co.

McAdoo, D. C., Agreen, R. W., Cheney, R. E., Douglas, B. C., Doyle, N. S., Miller, L., and Timmerman, E. L., 1990, Geosat/Geodetic mission geophysical data records: Format and contents: NOAA Tech. Memo..

McConathy, D. R., and Kilgus, C. C., 1987, The Navy Geosat Mission: An Overview: Johns Hopkins APL Technical Digest, **8**, no. 2, 170–175.

Rapp, R. H., and Pavlis, N. K., 1990, The development and analysis of geopotential coefficient models to spherical degree 360.: J. Geophys. Res., **95**, 21 885–21 991.

Roest, W. R., 1987, Seafloor spreading pattern of the North Atlantic between 10° and 40° N: Geologica Ultraiectina, **48**, 1–121.

Sandwell, D. T., 1991, Geophysical applications of satellite altimetry: Reviews of Geophysics, 132–137.

Sandwell, D. T., and D. C. McAdoo, 1990, High-accuracy, high-resolution gravity profiles from two years of the Geosat exact repeat mission: J. Geophys. Res., **95**, 3049–3060.

Welch, P. D., 1967, The use of the fast Fourier transform for estimation of power spectra: A method based on time averaging over short modified periodograms: IEEE Trans. Audio Electroacoust., **AU15**, 70–73.